AJNR

Dynamic Contrast-Enhanced MR Angiography and MR Imaging of the Carotid Artery: High-Resolution Sequences in Different Acquisition Planes

Shigeki Aoki, Hiroto Nakajima, Hiroshi Kumagai and Tsutomu Araki

AJNR Am J Neuroradiol 2000, 21 (2) 381-385
http://www.ajnr.org/content/21/2/381

AJNR Am J Neuroradiol 21:381–385, February 2000

Dynamic Contrast-Enhanced MR Angiography and MR Imaging of the Carotid Artery: High-Resolution Sequences in Different Acquisition Planes

Shigeki Aoki, Hiroto Nakajima, Hiroshi Kumagai, and Tsutomu Araki

BACKGROUND AND PURPOSE: **First-pass contrast-enhanced MR angiography has become the technique of choice for studying the carotid bifurcation, but this method has some limitations. We evaluated the clinical utility of performing 3D contrast-enhanced MR angiography in the axial plane immediately after performing angiography in the coronal plane.**

METHODS: **Cervical carotid arteries of 80 consecutive patients were studied on a 1.5-T MR imager with phased-array coils. Coronal 3D MR angiography was performed after administering a bolus injection of contrast material (20 mL) with automatic triggering. This was immediately followed by an axial acquisition. We measured carotid diameters on the contrast-enhanced MR angiograms as well as on intra-arterial digital subtraction angiograms according to established criteria. We also evaluated original source MR angiograms.**

RESULTS: **Angiograms obtained in the axial plane correlated better with the intra-arterial digital subtraction angiograms than did the coronal angiograms. When first-pass contrast-enhanced MR angiography was incomplete because of a failure of triggering, the second-phase acquisition provided sufficient image quality. Original source images suffered from ring artifacts, low axial resolution, and a low level of soft-tissue visualization. Axial-based source images showed flow-independent contrast filling to the patent lumen with sufficient visualization of plaque morphology, thickened arterial wall, and surrounding disease processes, such as tumors.**

CONCLUSION: **With the addition of a 1-minute second-phase 3D acquisition in a different plane immediately after first-pass contrast-enhanced MR angiography, one can obtain a more accurate depiction of the carotid bifurcation, insurance against failure of triggering, and diagnostic source images.**

Recently, imaging of the carotid artery has been the focus of considerable attention, primarily since the usefulness of carotid thromboendarterectomy was established by the North American Symptomatic Carotid Endarterectomy Trial (NASCET) (1) and by other investigations (2–4). Evaluation of the carotid bifurcation and proximal internal carotid arteries in these trials was achieved with conventional angiography, which has a complication rate of about 0.5% (5–7). To reduce risks related to conventional cerebral angiography, many noninvasive imaging approaches have been advocated, such as Doppler sonography (7), helical CT (8, 9), and noncontrast and contrast-enhanced MR angiography (10–12). Many researchers believe that not only the carotid artery diameter-based criteria, such as that of NASCET, but also other morphological changes on images may help to predict cerebral ischemia/infarction (13–24). Morphological changes in the arterial wall are clearly depicted on high-resolution noncontrast or contrast-enhanced MR images (17–25).

Dynamic contrast-enhanced MR angiography provides flow-independent anatomic information, and has many other advantages, including a short acquisition time and a minimal dephasing effect. This technique has rapidly become the procedure of choice for examining the aorta, neck, pelvis, and extremities (26–29). In particular, rapid circulation in the carotid territory requires a short acquisition time to avoid summation of venous structures. This short acquisition time leads to restrictions on the number of slices (limited second-order phase-encoding steps) and anisotropic voxels that can be obtained. When coronal 3D MR angiography is used to achieve an overview of the head and neck arteries, anteroposterior resolution is limited (usu-

Received March 9, 1999; accepted after revision September 13.

From the Department of Radiology, Yamanashi Medical University, 1110 Shimokato, Tamaho-cho, Nakakoma-gun, Yamanashi, 409-3898, Japan.

Presented in part at the annual meeting of the American Society of Neuroradiology, San Diego, May 1999.

Address reprint requests to Shigeki Aoki, MD.

ally by 2 to 5 mm). On the other hand, intimal thickening in the carotid bifurcation is frequently located at the posterolateral aspect of the carotid bulb (30, 31). The insufficient resolution in the anteroposterior direction might be a critical drawback in the diagnosis of carotid stenosis. Although special techniques, such as k-space segmentation with frequent sampling of lower spatial frequencies (3D time-resolved imaging of contrast kinetics) (10, 32) or the use of elliptical centric ordering (33), have been proposed for high-resolution contrast-enhanced MR angiography, these are not widely available.

Source images of first-pass MR angiography should have high differentiation between the contrast-filled vascular lumen and the surrounding structures in order to show the vessels. However, these images suffer from ring and other artifacts caused by the dynamic change of contrast material during acquisition, and visualization of surrounding structures, such as the arterial wall or adjacent tumor, has been limited. We postulated that if we added a relatively short 3D acquisition with sufficient resolution in the early phase of contrast injection (immediately after the first pass), we might obtain MR angiograms with adequate resolution in the anteroposterior direction as well as diagnostic source images in the region of the carotid bifurcation.

The purpose of this study was to ascertain the clinical usefulness of contrast-enhanced MR angiography in evaluations of the carotid bifurcation by using different acquisition planes and resolutions.

Methods

Cervical carotid arteries of 80 consecutive patients (57 male, 23 female; 16 to 88 years old; mean age, 57 years) were studied on a 1.5-T MR imager with phased-array coils. Patients were referred to our institution for contrast-enhanced MR imaging and/or MR angiography of the head and neck for cerebrovascular disease (35 patients), head and neck tumors (34 patients), or skull base and other tumors (11 patients). Thirty-three patients were also studied by conventional intraarterial digital subtraction angiography (IADSA).

MR imaging was performed on a 1.5-T imager with dual phased-array coils at the anterior neck and thoracolumbar spine or the torso (two 5-inch GP coils at both sides near the carotid bifurcations and one 5 × 11-inch square coil at the anterior neck). After intravenous injection of 20 mL of contrast material (gadopentetate dimeglumine), the first phase was obtained with a coronal 3D acquisition to show an overview of the arteries from the aortic arch to the circle of Willis, with a large field of view (FOV) and a short scan time (5.8/1.4 [TR/TE], 7.3-cm slab thickness, 14 slices, 30 × 30-cm FOV, 256 × 128 matrix [512 × 512 with interpolation], centric ordering in the k-space, and a scan time of 15 seconds). Automatic triggering was used. Bolus injection was done with a mechanical injector at a rate of 3 mL/s. The first phase was followed within 20 seconds by an axial 3D fast gradient-echo sequence (6.7/1.7, 2- to 3-mm thickness, 16- to 20-cm FOV, 256 × 224 matrix [512 × 512 with interpolation] with sequential view ordering in the k-space, an 84- to 112-mm slab thickness, and a scan time of 58 seconds) using a fat-saturation technique (spectrally selected inversion recovery pulse: TI = 30). Carotid bifurcations were covered within the scan fields. Contrast-enhanced MR angiograms were reconstructed and filmed from both phases with partial maximum intensity projection (MIP) and/or average targeting.

Using a loupe, one of the authors measured carotid bifurcations according to NASCET criteria (34) on the first- and second-phase MR angiograms and the IADSA images. The correlations (Pearson's correlation coefficient) were analyzed only when the diameter of the distal normal internal carotid artery was equal to or larger than that of the narrowed portion of the carotid bulb (ie, more than 0% stenosis by NASCET criteria). Two of the authors evaluated, by consensus, the image quality of the contrast-enhanced MR angiograms and the extent to which details of the carotid lumen, wall, and surrounding structures were depicted on the axial source images from the second phase.

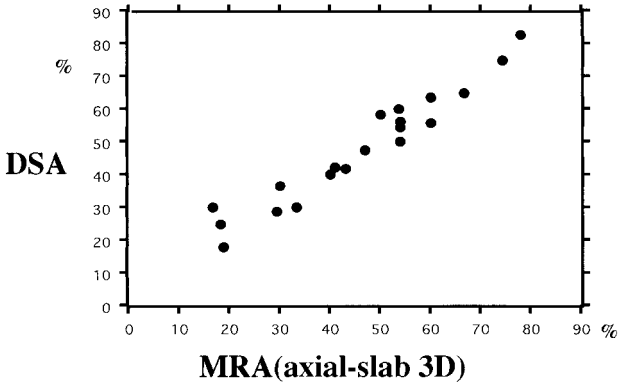

FIG 1. Correlation between second-phase (axial) 3D MR angiography and IADSA. Twenty carotid arteries in 15 patients were analyzed.

Results

Dynamic MR angiograms reconstructed from the second-phase (axial) 3D acquisition correlated well with IADSA images ($\gamma = .97$; $P < .001$) (Fig 1). Twenty carotid arteries of 33 patients who had both contrast-enhanced MR angiography and X-ray DSA showed more than 0% stenosis by NASCET criteria and were used for this analysis. Summation of the veins could be eliminated by the partial MIP/average targeting at the carotid bifurcation. Dynamic MR angiograms, which were reconstructed from the first-phase (coronal) 3D acquisition, also correlated with the DSA images ($\gamma = .71$; $P < .04$) (Fig 2), but not as well as those from the second-phase (axial) acquisition (Figs 2 and 3). Eighteen of 20 carotid arteries with matching characteristics were analyzed for this study (two arteries in one patient could not be used because of trigger failure during first-phase angiography). The first-pass contrast-enhanced MR angiograms were incomplete because of trigger failure or other mechanical difficulties in four of 80 cases. In all four of these failures, the second-phase angiograms were of satisfactory quality. On the other hand, the second-phase MR angiograms were occasionally incomplete (five cases) because of insufficient fat-saturation effects or patient movement. In these five cases, all the first-pass angiograms were of diagnostic quality.

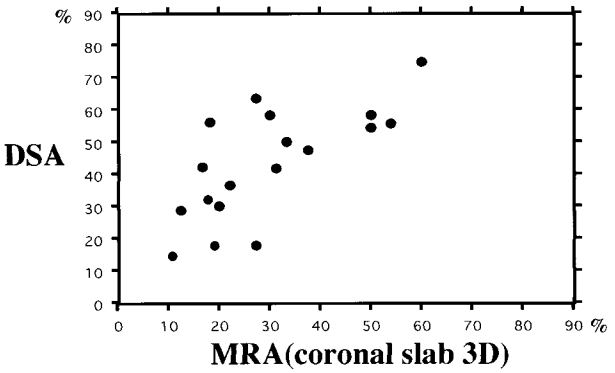

FIG 2. Correlation between first-pass (coronal) 3D MR angiography and IADSA. Eighteen carotid arteries in 14 patients were analyzed.

Axial 2D (source) images of the second-phase (axial) 3D sequence were of relatively good resolution without significant artifacts caused by rapid contrast changes during acquisition. On the axial images, a marked thickening of the enhancing wall was observed in patients with arteritis (Fig 4). Moderately eccentric/irregular thickening was observed in the area of atherosclerosis (Fig 3). One patient in whom irregular plaques were detected had a stroke 3 months later. In the regions surrounded by malignant tumors, details of the carotid wall and tumors were well demonstrated (Fig 5). However, original source images of the first-pass angiography suffered from ring artifacts and had low axial resolution.

A wide FOV for the first-pass (coronal plane) contrast-enhanced MR angiographic sequence was useful in delineating proximal occlusion of the common carotid artery and subclavian or vertebral stenosis/occlusion (Fig 4).

Discussion

Dynamic contrast-enhanced MR angiography provides information on flow-independent anatomic vascular structures; however, rapid circulation in the carotid territory usually requires precise bolus triggering with a centric data-filling technique into the k-space (centric order view). The scan triggering technique is essential in this centric data filling, and a test bolus injection for scan triggering (35), automatic triggering (36), or bolus monitoring by fluoroscopic MR imaging (33) is used to obtain good arterial phase contrast-enhanced MR angiograms. When bolus triggering fails for some reason, first-pass contrast-enhanced MR angiograms are easily deteriorated by an insufficient contrast filling to the arterial lumen or by contrast filling to the venous systems. DSA MR angiography, which continuously repeats 3D sequences with an acquisition time of about 5 seconds without triggering, has been proposed (10, 32). This appears to be a promising technique but requires a high performance gradient and special software. Our technique of adding a second phase is simple; it can be performed with a commercially available system and might contribute some alternative information when bolus triggering is insufficient.

Coronal first-pass 3D MR angiography can provide an overview of the carotid and vertebrobasilar systems from the aortic arch to the circle of Willis. This overview is essential in the assessment of cerebrovascular disorders, especially in the evaluation of atherosclerosis and arteritis, because these diseases are systemic and not limited to the carotid bifurcation. However, a wide FOV and a thick slab to cover a large volume of interest in a limited acquisition time usually leads to a large voxel size. The coronal slab typically has a thick anteroposterior diameter in anisotropic voxels. In other words, resolution in the anteroposterior direction is especially low in a standard (or normal) coronal 3D acquisition. Plaques at the carotid bifurcation almost always develop at the posterior aspect of the proximal internal carotid artery. To depict the posteroanteriorly protruded plaques, spatial resolution in this direction is essential. On a partial MIP image of the carotid bifurcation obtained from a standard coronal 3D acquisition, details of the luminal narrowing were obscured owing to this large voxel and low anteroposterior resolution. Several techniques to obtain a high-resolution 3D data set (near isotropic voxel) in one short acquisition have been proposed, including segmented k-space filling (10, 32) or an elliptical centric order view (33). These sophisticated methods appear to be promising, but are not widely available at this time. In addition, centric data fitting to the k-space with rapidly changing contrast during the acquisition deteriorates the quality of the source image by ringing, blurring, or ghosting artifacts, and so on. First-pass contrast-enhanced MR angiography provides excellent contrast between the enhanced lumen and the surrounding soft tissue, but, at the same time, eliminates soft tissue (ie, background) visualization to a considerable degree. Source images or reconstructed slices from the first-pass angiography are insufficient for diagnostic evaluation because they cannot show pathologic changes of the surrounding soft tissue.

Axial source images (with sufficient diagnostic quality) provided us with useful information beyond that concerning intraluminal morphology, because they clearly showed thickening of the wall in arteritis and tumors surrounding the carotid artery. Plaque morphology was also observed; and, in one such instance, a patient who had irregular plaque formation had a stroke 3 months after MR angiography. Further study might reveal that, in addition to the luminal diameter, plaque morphology may be associated with stroke risk. Several studies of atherosclerotic plaques on high-resolution MR images (17–25) have found an excellent correlation between MR and pathologic findings. In atherosclerosis or aortitis, neovascularity of the diseased wall (proliferation of the vasa vasorum) has been reported as a possible cause of intramural dissec-

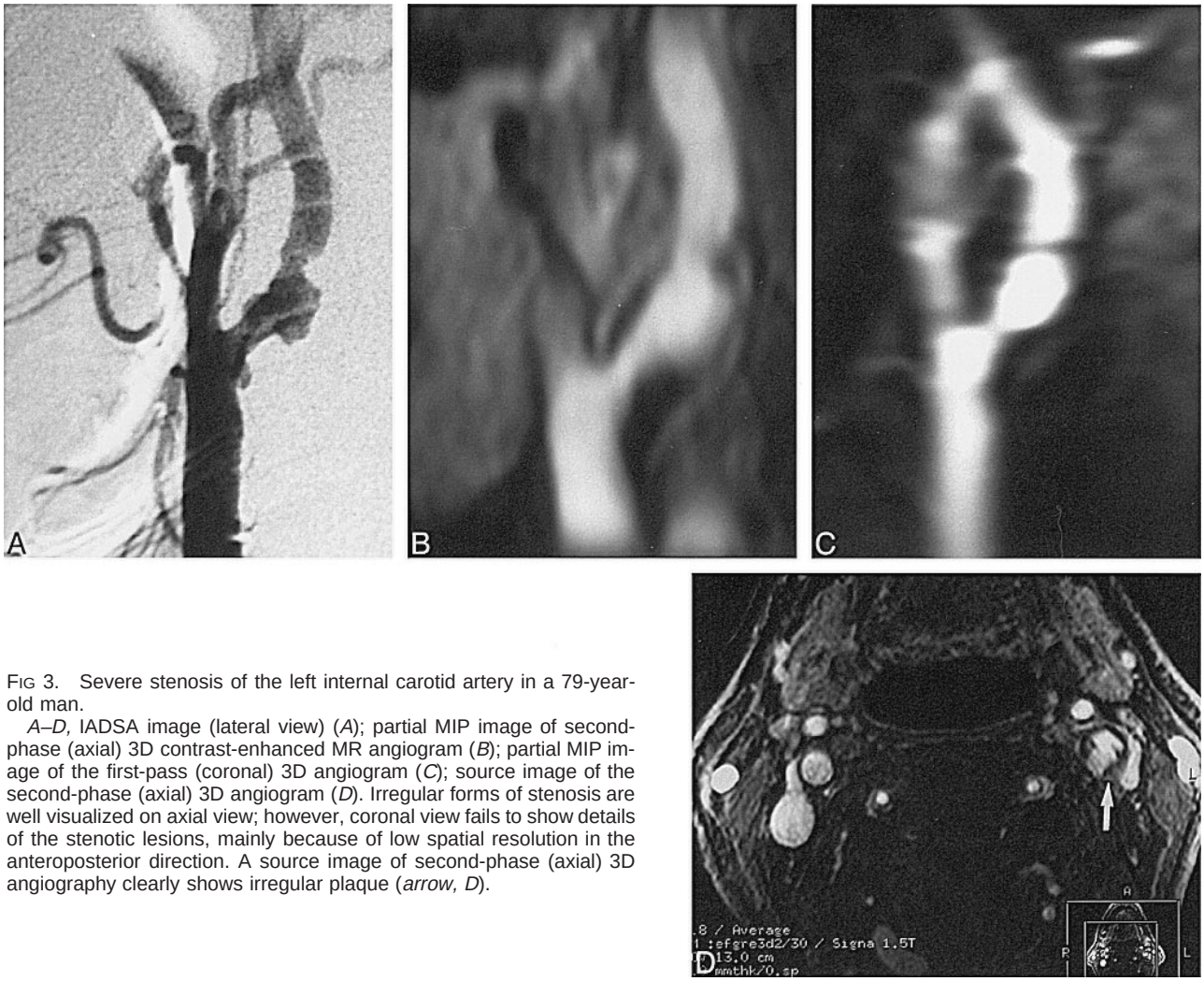

FIG 3. Severe stenosis of the left internal carotid artery in a 79-year-old man.

A–D, IADSA image (lateral view) (*A*); partial MIP image of second-phase (axial) 3D contrast-enhanced MR angiogram (*B*); partial MIP image of the first-pass (coronal) 3D angiogram (*C*); source image of the second-phase (axial) 3D angiogram (*D*). Irregular forms of stenosis are well visualized on axial view; however, coronal view fails to show details of the stenotic lesions, mainly because of low spatial resolution in the anteroposterior direction. A source image of second-phase (axial) 3D angiography clearly shows irregular plaque (*arrow, D*).

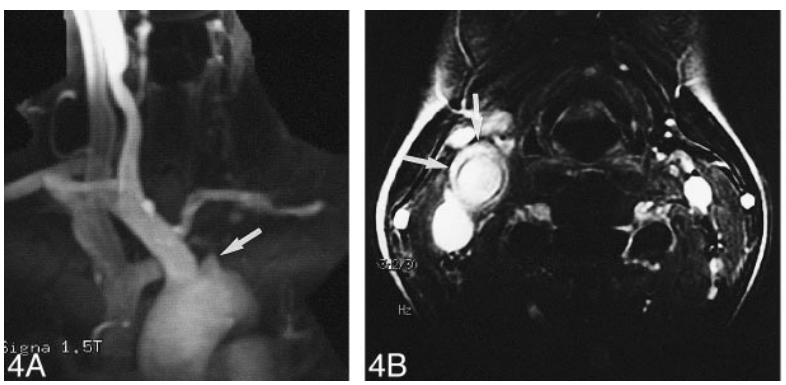

FIG 4. Marked thickening of left common carotid wall in a 35-year-old woman with arteritis.

A, First-pass (coronal) 3D contrast-enhanced MR angiography shows occlusion of the left common carotid artery (*arrow*) and the left subclavian artery. The right common and internal carotid arteries are dilated.

B, Source image of second-phase (axial) MR angiography shows marked thickening and enhancement of the wall of the common carotid artery (*arrows*).

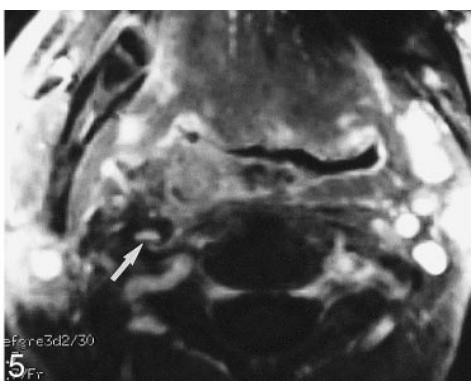

FIG 5. Source image of second-phase (axial) MR angiography shows invasion of the left internal carotid artery by nasopharyngeal carcinoma (*arrow*).

tion and hemorrhage (24). Several researchers have reported that the enhancement of the arterial wall on MR images is related to atherosclerosis-like neovascularity of the wall (24, 25, 37). Wall thickening and enhancement were important findings in arteritis, as well as dissection (38–40). In our study, wall thickness and vascularity of the wall itself were easily observed with contrast enhancement, and we could reconstruct the MR angiogram.

Conclusion

With the addition of a 1-minute second-phase 3D acquisition in a different plane immediately after first-pass contrast-enhanced MR angiography, one can obtain a more accurate depiction of the carotid bifurcation, insurance against failure of triggering, and diagnostic source images.

References

1. North American Symptomatic Carotid Endarterectomy Trial Collaborators. **Beneficial effect of carotid endarterectomy in symptomatic patients with high-grade carotid stenosis.** *N Engl J Med* 1991;325:445–453
2. Executive Committee for the Asymptomatic Carotid Atherosclerosis Study. **Endarterectomy for asymptomatic carotid artery stenosis.** *JAMA* 1995;273:1421–1428
3. European Carotid Surgery Trialists' Collaborative Group. **MRC European Carotid Surgery Trial: interim results for symptomatic patients with severe (70–99%) or with mild (0–29%) carotid stenosis.** *Lancet* 1991;337:1235–1243
4. European Carotid Surgery Trialists' Collaborative Group. **Endarterectomy for moderate symptomatic carotid stenosis: interim results from the MRC European Carotid Surgery Trial.** *Lancet* 1996;347:1591–1593
5. Chaturvedi S, Policherla PN, Femino L. **Cerebral angiography practices at US teaching hospitals: implications for carotid endarterectomy.** *Stroke* 1997;28:1895–1897
6. Heiserman JE, Dean BL, Hodak JA, et al. **Neurologic complications of cerebral angiography.** *AJNR Am J Neuroradiol* 1994; 15:1401–1407
7. Polak JF, Kalina P, Donaldson MC, et al. **Carotid endarterectomy: preoperative evaluation of candidates with combined Doppler sonography and MR angiography, work in progress.** *Radiology* 1993;186:333–338
8. Schwartz RB, Jones KM, Chernoff DM, et al. **Common carotid artery bifurcation: evaluation with spiral CT, work in progress.** *Radiology* 1992;185:513–519
9. Dillon EH, van Leeuwen MS, Fernandez MA, Eikelboom BC, Mali WP. **CT angiography: application to the evaluation of carotid artery stenosis.** *Radiology* 1993;189:211–229
10. Willig DS, Turski PA, Frayne R, et al. **Contrast-enhanced 3D MR DSA of the carotid artery bifurcation: preliminary study of comparison with unenhanced 2D and 3D time-of-flight MR angiography.** *Radiology* 1998;208:447–451
11. Remonda L, Heid O, Schrogh G. **Carotid artery stenosis, occlusion, and pseudo-occlusion: first-pass, gadolinium-enhanced, three-dimensional MR angiography, preliminary study.** *Radiology* 1998;209:95–102
12. Slosman F, Stolpen AH, Lexa FJ, et al. **Extracranial atherosclerotic carotid artery disease: evaluation of non-breath-hold three-dimensional gadolinium-enhanced MR angiography.** *AJR Am J Roentgenol* 1998;170:489–495
13. Fisher M, Blumenfeld AM, Smith TW. **The importance of carotid artery plaque disruption and hemorrhage.** *Arch Neurol* 1987;44:1086–1089
14. Sitzer M, Muller W, Siebler M, et al. **Plaque ulceration and lumen thrombus are the main sources of cerebral microemboli in high-grade internal carotid artery stenosis.** *Stroke* 1995;26: 1231–1233
15. Eliasziw M, Streifler JY, Fox AJ, et al. **Significance of plaque ulceration in symptomatic patients with high-grade carotid stenosis.** *Stroke* 1994;25:304–308
16. Streifler JY, Eliasziw M, Fox AJ, et al. **Angiographic detection of carotid plaque ulceration: comparison with surgical observations in a multicenter study, North American Symptomatic Carotid Endarterectomy Trial.** *Stroke* 1994;25:1130–1132
17. Wasserman BA, Haacke EM, Li D. **Carotid plaque formation and its evaluation with angiography, ultrasound, and MR angiography.** *J Magn Reson Imaging* 1994;4:515–527
18. Gold GE, Pauly JM, Glover GH, Moretto JC, Macovski A, Herfkens RJ. **Characterization of atherosclerosis with a 1.5-T imaging system.** *J Magn Reson Imaging* 1993;3:399–407
19. Toussaint JF, La Muraglia GM, Southern JF, Fuster V, Kantor HL. **Magnetic resonance images: lipid, fibrous, calcified, hemorrhagic, and thrombotic components of human atherosclerosis in vivo.** *Circulation* 1996;94:932–938
20. Behling W, Tubbs HK, Cockman MD, Jelinski LW. **Stroboscopic NMR microscopy of the carotid artery.** *Nature* 1989;341:321–323
21. Yuan C, Tsuruda JS, Beach KN, et al. **Techniques for high-resolution MR imaging of atherosclerotic plaque.** *J Magn Reson Imaging* 1994;4:43–49
22. Yuan C, Murakami JW, Hayes CE, et al. **Phased-array magnetic resonance imaging of the carotid artery bifurcation: preliminary results in healthy volunteers and a patient with atherosclerotic disease.** *J Magn Reson Imaging* 1995;5:561–565
23. Martin AJ, Ryan LK, Gotlieb AI, Henkelman RM, Foster FS. **Arterial imaging: comparison of high-resolution US and MR imaging with histologic correlation.** *Radiographics* 1997;17: 189–202
24. Lin W, Abendschein DR, Haacke EM. **Contrast-enhanced magnetic resonance angiography of carotid arterial wall in pigs.** *J Magn Reson Imaging* 1997;7:183–190
25. Aoki K, Aoki S, Shirasu M, et al. **Evaluation of the wall of the carotid bifurcation with high-resolution dynamic MR imaging.** *Radiology* 1996;201(P):134
26. Leung DA, McKinnon GC, Davis CP, Pfammatter T, Krestin GP, Debatin JF. **Breath-hold, contrast-enhanced, three-dimensional MR angiography.** *Radiology* 1996;200:569–571
27. Prince MR. **Gadolinium-enhanced MR aortography.** *Radiology* 1994;191:155–164
28. Revel D, Loubeyre P, Delignette A, Douek P, Amiel M. **Contrast-enhanced magnetic resonance tomoangiography: a new imaging technique for studying thoracic great vessels.** *Magn Reson Imaging* 1993;11:1101–1105
29. Alley MT, Shifrin RY, Pelc NJ, Herfkens RJ. **Ultrafast contrast-enhanced three-dimensional MR angiography: state of the art.** *Radiographics* 1998;18:273–285
30. Ku DN, Giddens DP, Zarins CK, Glagov S. **Pulsatile flow and atherosclerosis in the human carotid bifurcation.** *Atherosclerosis* 1985;5:293–302
31. Lasjaunias P, Berenstein A. ***Surgical Neuroangiography.*** Book 1. New York: Springer;1987:1–4
32. Korosec FR, Frayne R, Grist TM, Mistretta CA. **Time-resolved contrast-enhanced 3D MR angiography.** *Magn Reson Med* 1996;36:345–351
33. Wilman AH, Riederer SJ, Huston J III, Wald JT, Debbins JP. **Arterial phase carotid and vertebral artery imaging in 3D contrast-enhanced MR angiography by combining fluoroscopic triggering with an elliptical centric acquisition order.** *Magn Reson Med* 1998;40:24–35
34. Fox AJ. **How to measure carotid stenosis.** *Radiology* 1993;186: 316–318
35. Kim JK, Farb RI, Wright GA. **Test bolus examination in the carotid artery at dynamic gadolinium-enhanced MR angiography.** *Radiology* 1998;206:283–289
36. Prince MR, Chenevert TL, Foo TK, Londy FJ, Ward JS, Maki JH. **Contrast-enhanced abdominal MR angiography: optimization of imaging delay time by automating the detection of contrast material arrival in the aorta.** *Radiology* 1997;203:109–114
37. Aoki S, Shirouzu I, Sasaki Y, et al. **Enhancement of the intracranial arterial wall at MR imaging: relationship to cerebral atherosclerosis.** *Radiology* 1995;194:477–481
38. Park JH, Chung JW, Im JG, Kim SK, Park YB, Han MC. **Takayasu arteritis: evaluation of mural changes in the aorta and pulmonary artery with CT angiography.** *Radiology* 1995;196: 89–93
39. Sharma S, Sharma S, Taneja K, Gupta AK, Rajani M. **Morphologic mural changes in the aorta revealed by CT in patients with nonspecific aortoarteritis (Takayasu's arteritis).** *AJR Am J Roentgenol* 1996;167:1321–1325
40. Hosoya T, Watanabe N, Yamaguchi K, Kubota H, Onodera Y. **Intracranial vertebral artery dissection in Wallenberg syndrome.** *AJNR Am J Neuroradiol* 1994;15:1161–1165